ACS APPLIED MATERIALS & INTERFACES

Research Article

www.acsami.org

Lead Iodide Thin Film Crystallization Control for High-Performance and Stable Solution-Processed Perovskite Solar Cells

Lijun Yang, Jingchuan Wang, and Wallace Woon-Fong Leung*

Department of Mechanical Engineering, The Hong Kong Polytechnic University, Hung Hom, Hong Kong

Supporting Information

ABSTRACT: PbI_2 thin film crystallization control is a prerequisite of high-quality perovskite thin film for sequentially solution-processed perovskite solar cells. An efficient and simple method has been developed by adding HCl to improve perovskite thin film quality, and an efficiency of 15.2% is obtained. This approach improves coverage, uniformity, and stability of pervoskite thin film.

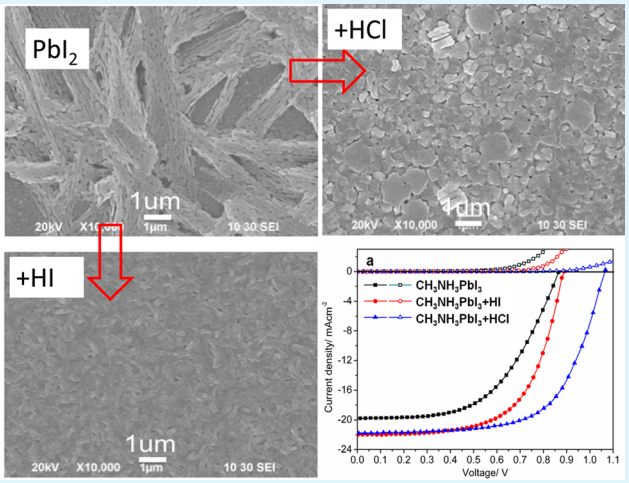

KEYWORDS: *perovskite, thin film quality, additive, stability*

INTRODUCTION

Low-cost solution-processable solar cells, including organic photovoltaic (OPV) and dye-sensitized solar cells (DSSC), are attractive to researchers in photovoltaics (PV). Currently, the power conversion efficiency (PCE) for OPV and DSSC at 11+ and 13+%, respectively, seems to have reached the ceiling for these devices. This might be related to the thermodynamic loss caused by tightly bounded exciton and poor mobility of the charge carrier. In contrast, the solution-processed perovskite solar cell has stirred up research enthusiasm worldwide since its pioneering.[1−5] This is especially because of the recently reported impressive PCE of 20.1%.[6] Low-temperature processing (<100 °C), solution processability, and compatibility with the current thin film PV production technology are all attractive advantages for commercializing the perovskite solar cell in the near future.

In an ideal perovskite solar cell, the crystal $CH_3NH_3PbX_3$ (X = Cl, Br, and I) works as a light-absorbing layer sandwiched between the electron- and hole-transport layers (abbreviated as ETL and HTL, respectively). TiO_2 is typically used as ETL, and Spiro-MeOTAD is used as HTL. In pursuit of high efficiency,[7] much effort has been devoted to improving the device performance, such as modifying the device configuration, and to controlling the physical properties and morphology of the active layer.[8−11] To date, most of the state-of-the-art perovskite solar cells utilize a metal oxide mesoporous scaffold to support a uniform, flat light-absorbing layer.[2−4] Whether it takes on the thin-film- or scaffold-based configuration, a high-quality perovskite thin film is the prerequisite for a high-performance solar cell. Investigations carried out by Snaith and co-workers[12] indicated that a high-quality perovskite layer by vapor deposition can produce a solar cell with efficiency up to 15.4%, which is approximately 35% higher than that of solution-phase-fabricated devices in the absence of mesoporous scaffold. Because of the highly sensitive dependence of the perovskite thin film morphology on crystallization by solution processing, the precursor composition and concentration are critical factors. Motivated by the desire to improve the perovskite thin film quality using a one-step solution-phase approach, Jen[13] and Snaith[14] added 1,8-diiodooctane (DOI) and hydroiodic acid (HI), respectively, into formamidinium iodide (FAI) together with PbI_2 precursor solution in *N*,*N*-dimethylformamide (DMF) to improve perovskite crystallization on the dense layer. Xiao et al., Wu et al., and Heo et al. also did some meanful work in this direction.[15−17]

Using a two-step solution deposition process, our objective in this study is to obtain a thin film comparable to that obtained from vapor deposition.[8] In conjunction, we have launched a systematic investigation on the effect of halogen acid additives, i.e., hydroiodic acid (HI) and hydrochloric acid (HCl), on (i)

Received: February 5, 2015
Accepted: June 25, 2015
Published: June 25, 2015

DOI: 10.1021/acsami.5b01049
ACS Appl. Mater. Interfaces 2015, 7, 14614−14619

PbI_2 crystallization, (ii) perovskite morphology, (iii) device performance, and (iv) stability of the solar cell. We will demonstrate a simple means of incorporating HCl into PbI_2 precursor solution, with the consequence that it inhibits the rod-shape PbI_2 crystallization and promotes homogeneous nucleation and crystal growth, further improving uniformity and coverage of the perovskite thin film on the dense TiO_2 layer. With a simple HCl additive, a high efficiency of 15.2% has been attained with the planar-heterojunction perovskite solar cell under AM1.5G standard solar simulation with excellent device stability under room temperature yet with relative humidity (RH%) in excess of 80%.

RESULTS AND DISSCUSSION

Instead of a one-step solution phase approach, a two-step solution process method was adopted herein to fabricate a perovskite layer $CH_3NH_3PbI_3$.[4,18] A liquid drop of the PbI_2 solution was deposited and spin-coated onto a well-prepared TiO_2 dense layer precoated on the laser-patterned FTO glass. This was followed by immersion of the dried substrate in a CH_3NH_3I solution. Subsequently, an HTL composed of Spiro-MeOTAD was spin-coated onto the perovskite thin film. Lastly, MoO_3 and Ag were evaporated onto the HTL to form an electron-blocking layer and a counter electrode, respectively, thereby completing the device. Figure 1a,b shows the cross-sectional SEM image of the perovskite solar cells and the related device architecture, respectively. The interfacial MoO_3 layer was used to strengthen the electron-blocking effect because it has an aligned energy level and is also an environmentally inert material. The thickness of the perovskite layer is about 350−450 nm. Of great interest is that the entire crystalline grain, sandwiched between HTL and ETL, is a single crystal in an unidirection (i.e., vertical as shown in Figure 1a). This is also along the electron/hole transport layer without introducing additional boundaries that can lead to undesirable scattering effects and electron−hole recombination taking place at grain boundaries as the charge carriers are transported across the two electrodes.

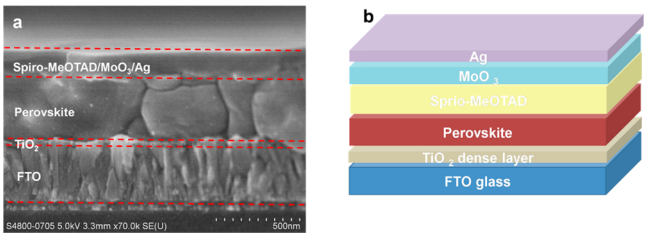

Figure 1. Device configuration of the planar heterojunction perovskite solar cell adopted in this study. (a) Cross section SEM of the solar cell. (b) Device architecture.

As a departure from the studies of Jen and Snaith of adding additives directly to the perovskite precursor solution by a one-step method, we take a well-controlled, two-step sequential deposition route to prepare controlled perovskite crystals, thereby improving the morphology of perovskite thin film. In our first step, we control the mechanism of crystallization (size and shape of crystals) of PbI_2 thin film by using halogen acid to influence the crystal growth, in particular, inhibiting the linear growth along the PbI_2 axis but rather encouraging crystal growth along the entire boundary of the crystal. The resulting hexagonal-plate-shaped crystals of PbI_2 provide a uniform coverage of the TiO_2 dense layer. In the second step, when the organic phase is introduced, a thin film made of uniformly sized perovskite crystals forms, providing excellent morphology and coverage of the dense TiO_2 layer. Both halogen acid additives, HCl and HI, are in the halogen family with the advantage that they do not introduce alien atoms in the host matrix. The SEM images of PbI_2 thin films without and with additives and the corresponding perovskite layers are shown in Figure 2 a−f. Figure 2a is an image of PbI_2 thin film on the TiO_2 dense layer without additive, which serves as the benchmark. Figure 2b,c shows the evolution of PbI_2 thin film morphology on the TiO_2 dense layer after adding 2.5 vol % HI and HCl, respectively, to 1 M PbI_2 solution. The material domain of PbI_2 crystal formed by "raw" PbI_2 solution has a very large aspect ratio (aspect ratio = d_{max}/d_{min}, with d being the characteristic dimension of the structure), which means that the compactness or coverage of the thin film formed by these rod-shaped structures (1 nm wide by tens of microns in length) cannot be high, providing at best 70−80% coverage of the TiO_2 dense layer (Figure 2a). However, the coverage of the thin films can be remarkably improved by adding HI and HCl to the PbI_2 solution because the morphology of PbI_2 transforms from rod-shaped crystals into hexagonal-plate crystals (Figure 2b,c). The compacted PbI_2 thin films cover most of TiO_2 dense layer, which benefits the morphology of the as-deposited perovskite thin film, shown in Figure 2e,f, respectively. Given the uniform shape (in all orientations) and size (1 nm and less) of the perovskite crystals, the coverage of pristine perovskite thin film on the TiO_2 dense layer was increased from approximately 80 to 100%. It is worth noting that the quality of our solution-processed perovskite thin film can be comparable to that obtained by vapor deposition.[8] As demonstrated by the large-scale SEM in the Supporting Information (Figure S1), the absence of voids in the perovskite thin film with the HCl additive is in strong contrast to voids (or uncovered areas) present on the TiO_2 dense layer in the case of precursor without additives (Figure 2a,d). The voids affect significantly the performance of the thin film solar cells because the defects/voids in the light absorption layer create serious short-circuiting, and they also serve as trapping sites for electron−hole recombination.

Using halogen acid additives in PbI_2 solution, we can control PbI_2 crystallzation and growth in thin film during spin-coating. The morphology of PbI_2 thin film is sensitive to the solution concentration and composition. Addition of HI and HCl into the PbI_2 in DMF solution can improve remarkably the solubility of PbI_2 in DMF solvent. Indeed, 1 M of PbI_2 in DMF solution with 2.5 vol % HCl additive can be kept stably over a week at room temperature. This contrasts with the pristine PbI_2 solution with an obvious crystallization over time (Figure S2). In fact, this undersaturated PbI_2/DMF solution with HCl additive will slow down the crystallization rate that facilitates more homogeneous nucleation and growth of the PbI_2 thin film. Furthermore, XRD patterns of PbI_2 thin film with and without additives are examined and shown in Figure 2g. The crystals generated in the PbI_2 thin film with additives (both HI and HCl) oriented with the (001) plane that parallels to the substrate, whereas for PbI_2 thin film without additive, it can be observed that there is another peak originating from the (102) plane.[19] Therefore, with additive, especially HCl, the crystallization and coverage of PbI_2 thin film can be improved, which subsequently improves the morphology of the perovskite thin film.

DOI: 10.1021/acsami.5b01049
ACS Appl. Mater. Interfaces 2015, 7, 14614−14619

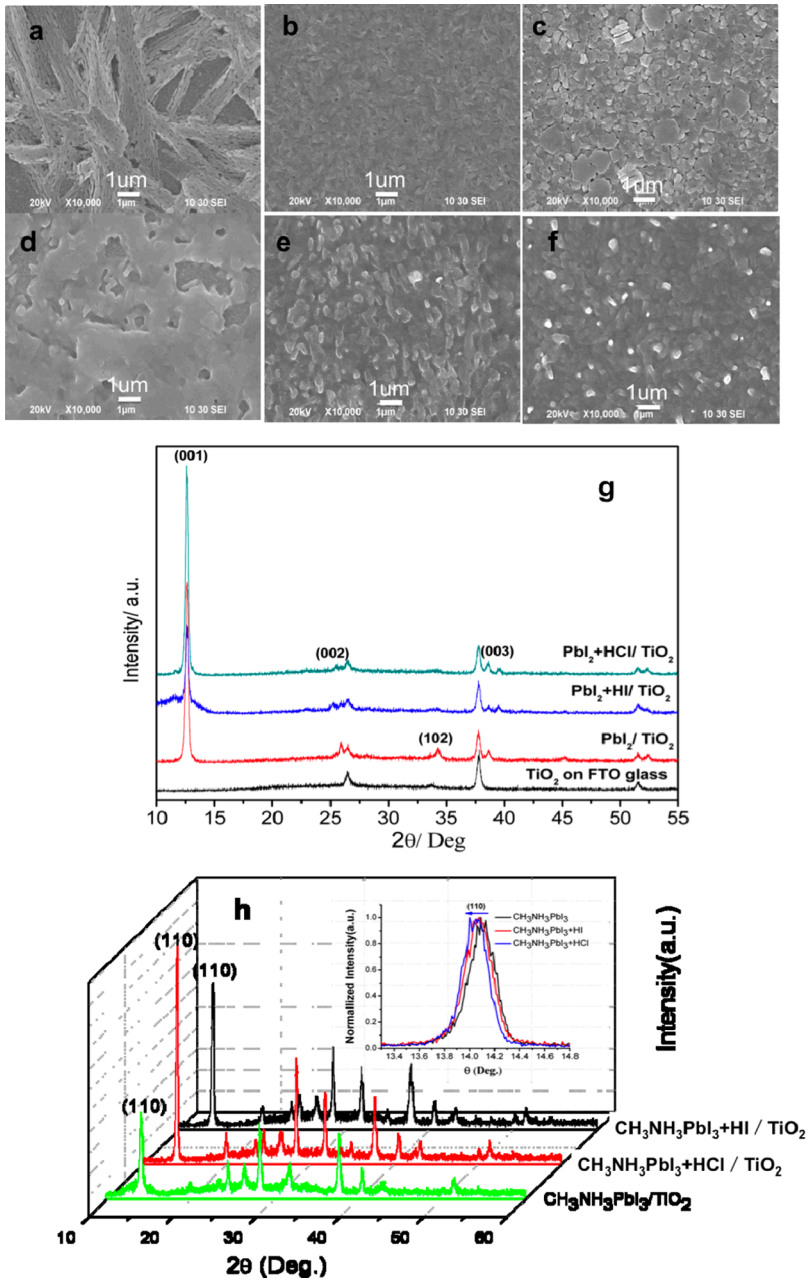

Figure 2. Topographic SEM images and XRD patterns of PbI_2 thin film and corresponding perovskite layers. (a–c) Pristine PbI_2, PbI_2 with HI, and PbI_2 with HCl on the TiO_2 dense layer coated FTO, respectively. (d–f) $CH_3NH_3PbI_3$, $CH_3NH_3PbI_3$+HI, and $CH_3NH_3PbI_3$+HCl, respectively, after sequentially reacting with CH_3NH_3I. (g) XRD patterns of PbI_2 thin films on the TiO_2 dense layer coated on FTO glass. (h) XRD patterns of the solution-processed perovskite thin films, pristine perovskite, the perovskite with HI added, and the perovskite with HCl added. Inset shows the shift of (110) peak.

For the cases with addition of HCl, rod-shaped PbI_2 crystals (without halogen acid) have been changed into hexagonal-plate-like crystal architecture. During the spin-coating process, rod-shaped crystallization from the supersaturation PbI_2/DMF solution with a high volatility is more likely formed from the effect of centrifugal force, as shown in Figure 2a, whereas with HCl additive, solvent evaporation dictates the PbI_2 crystallization from the undersaturated solution during and post spin-coating process. As a result, hexagonal-plate crystal architecture is formed as seen in Figure 2c.

The planar-heterojunction perovskite solar cells of pristine perovskite and perovskite with halogen acid additives, i.e., HI and HCl, have been fabricated. The best-performing current density–voltage (J–V) characteristics of the devices without and with additives are shown in Figure 3a, and related photovoltaic parameters are listed in Table 1. (The average performance parameters are listed in Table S1.) These are based on measurements obtained under 100 mW cm^{-2} AM1.5G standard solar spectrum. The device with 2.5 vol % HI additive reached a promising PCE of 12.17%, nearly 30% enhancement in PCE when compared with the that of the control device (9.35%). In contrast, a high efficiency of 14.8% was obtained from the device with 2.5 vol % HCl additive, an impressive 58% enhancement when compared with that of the pristine device. It is worth noting that the improved performance (30%) by introducing HI is mainly due to

DOI: 10.1021/acsami.5b01049
ACS Appl. Mater. Interfaces 2015, 7, 14614–14619

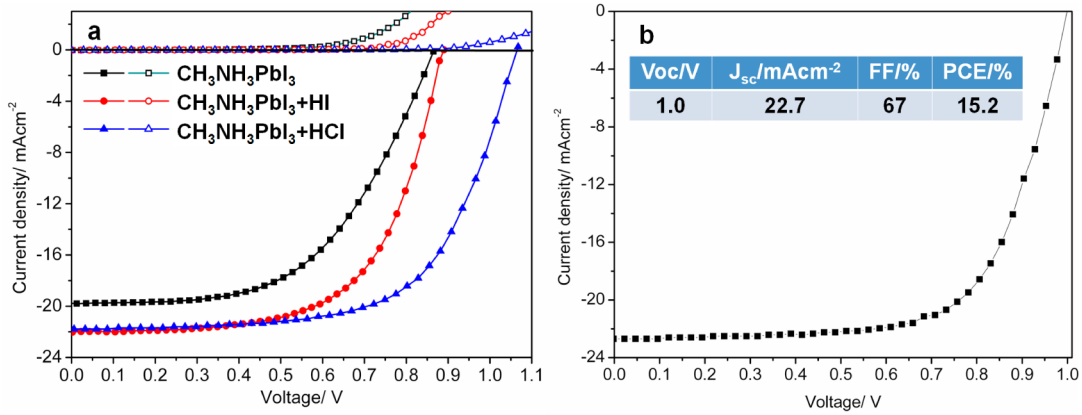

Figure 3. (a) $J-V$ curves measured under 100 mW cm^{-2} AM1.5G illumination (curves with solid symbols) and in the dark (curves with hollow symbols) for the perovskite and perovskite with HI and HCl added devices. (b) $J-V$ curve for the optimized device with HCl added.

Table 1. Performance of the Studied Perovskite Solar Cells under AM 1.5 G Illumination

	V_{oc} (V)	J_{sc} (mA cm^{-2})	FF (%)	PCE (%)	J_{sc} (mA cm^{-2})[a]
$CH_3NH_3PbI_3$	0.87	18.94	57	9.4	17.50
$CH_3NH_3PbI_3$+HI	0.89	22.02	62	12.2	20.48
$CH_3NH_3PbI_3$+HCl	1.06	21.77	64	14.8	21.24

[a]Obtained from EQE.

increased short-current density (J_{sc}) from 18.94 to 22.02 mA cm^{-2}. However, further improved PCE (58% enhancement) in the device with HCl additive is attributed not only to the increased J_{sc} but also to the improved open-circuit voltage (V_{oc}) from 0.87 to 1.06 V. A staggeringly high efficiency of 15.2% has been obtained (Figure 3b) upon further optimization of the thickness of the perovskite layer and concentration of HCl additive. The optimization of layer thickness by changing spin-coating speed and hysteresis phenomenon during test measurement are depicted in Figures S3 and S4, and the forward bias to short-circuit scan between two curves was taken for our PCE value because it gives a close estimate for the steady-state efficiency.[20] This significant enhancement in performance with use of additives should be attributed to the improved thin film quality,[21] which provides uniform coverage of the TiO_2 dense layer, thereby maximizing energy harvesting and minimizing short-circuiting because of voids in the dense layer.

Interestingly, the improved thin film quality and uniform crystals in the perovskite layer with halogen acid additives can further enhance solar absorbance. Three types of thin film, pristine perovskite, perovskite with HI and HCl additives, were prepared on TiO_2 dense layer by the same procedure with approximately the same thickness. In Figure 4a, the absorbance of the perovskite thin films reveals a sequential increase over the entire visible solar spectrum range from the reference sample to the perovskite with HI additive and to the perovskite with HCl additive. This is consistent with the increased performance of external quantum efficiency (EQE) as shown in Figure 4b. The increased absorbance can be contributed to the improved surface coverage and crystallinity of perovskite thin films with additives. The improved crystallinity can be observed in XRD pattern (Figure. 2h). The intensity of the main peak (110) of $CH_3NH_3PbI_3$ at 14.11° shows a remarkable increase when introducing additives (both HI and HCl).[9] A close examination of the main peak (110) reveals a blueshift caused by HCl additive (inset, Figure 2h). This is probably due to the introduction of Cl atoms in the $CH_3NH_3PbI_3$ lattice causing an expansion of the lattice structure, despite the fact that Cl cannot be detected by the XPS measurement, as seen in Figure S5.

So far, it has been demonstrated that improvement of the perovskite thin film coverage, uniformity, and crystallinity can be realized by introducing halogen acid additives, i.e., HCl and HI especially the former. As a new organic–inorganic hybrid

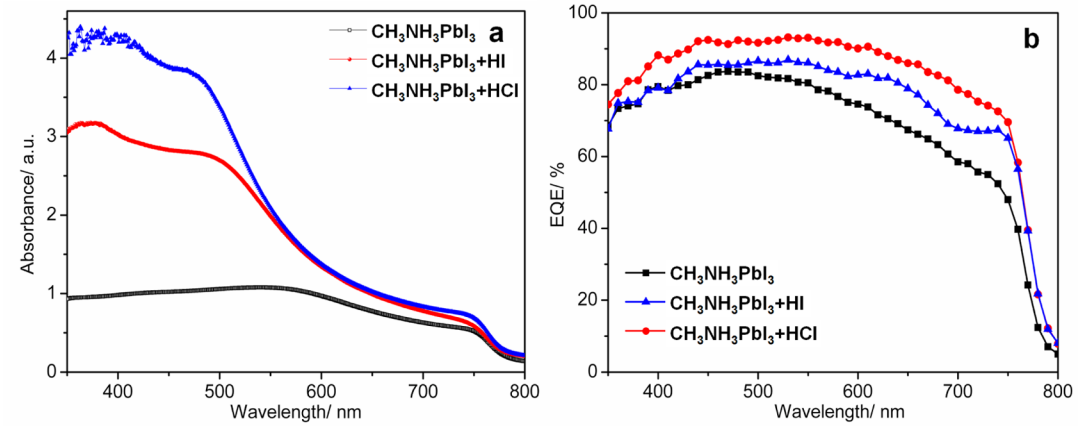

Figure 4. (a) UV–vis absorbance spectra. (b) External quantum efficiency (EQE).

DOI: 10.1021/acsami.5b01049
ACS Appl. Mater. Interfaces 2015, 7, 14614–14619

perovskite member in the photovoltaic family, the stability of device is an important issue for its potential application. Furthermore, the introduction of Cl atoms is expected to improve the stability of $CH_3NH_3PbI_3$ because of the larger electron negativity of chloride as compared to that of iodide. In essence, it strengthens the metal−halogen bond and keeps the material more stable. The longitudinal follow-up on the photovoltaic parameters of devices without and with HI/HCl additives can be found in Figure 5a. These devices are

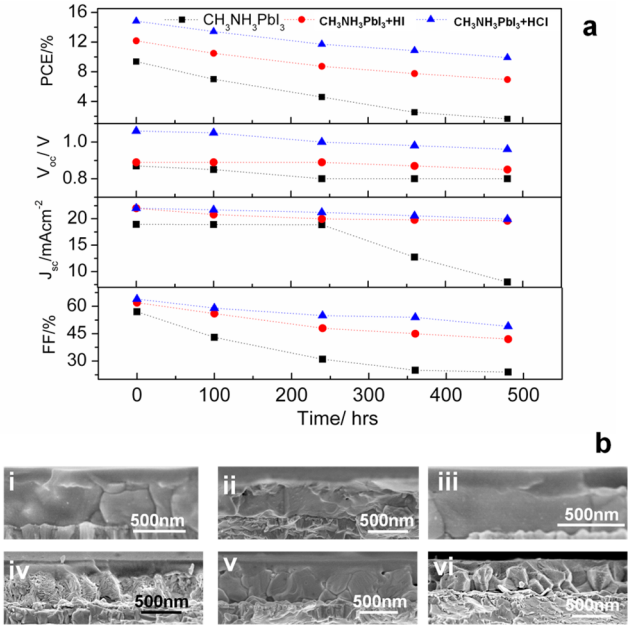

Figure 5. (a) Stability on performance of the solution-processed planar heterojunction perovskite solar cells exposed in air at room temperature and over 80 RH%. (b) Cross section SEM images. Freshly prepared devices of pristine perovskite, the perovskite with HI added, and the perovskite with HCl added (i−iii, respectively). Corresponding devices are exposed to air with 80 RH%, without encapsulation, after 1 week (iv−vi, respectively).

encapsulated simply by the epoxy glue covered with glass slides and maintained in air at room temperature and over 80 RH% . It is well-known that perovskite material is sensitive to water vapor.[2,5] Monitoring the test devices in a relatively high humidity environment facilitates the investigation into the stability of device in an accelerated time frame. The device with additive shows some degraded PCE value over 500 h, 43% for HI additive and 35% for HCl additive; however, the performance of the pristine perovskite solar cell decreases 50% after 250 h and 82% after 500 h. Besides PCE, evolution of other important photovoltaic parameters can also be observed in Figure 5a. These include the degradation of J_{sc} and fill factor (FF) over time, which are the major reasons for decrease of PCE. It is to be expected that the mobility dropped off as a result of deterioration on the perovskite thin film quality. It means that perovskite with additive has not only improved thin film quality but also enhanced stability of the device, especially with HCl additive. To get an in-depth understanding of improved stability of the device, time-resolved morphology analyses were carried out and recorded with cross-sectional SEM, as present in Figure 5b. Figure 5b shows cross-sectional SEM images i−iii of fresh samples corresponding to pristine perovskite, perovskite with HI additive, and perovskite with HCl additive, respectively, whereas Figure 5b shows corresponding SEM images iv−vi of these same materials in air without encapsulation after 1 week. It can be clearly seen that the pristine perovskite crystals degraded into crystals with stripes or streaks on their surfaces. The perovskite domains with HI additive changed slightly, whereas the perovskite domains with HCl additive seemed unchanged under the same harsh conditions. This interesting observation can be further supported by the XPS measurement (Table S2). The atomic concentration of oxygen (from environment; i.e., O_2 and H_2O in air and XPS chamber) in perovskite thin film is as much as 50% lower than that in pristine perovskite thin film. The lower the water vapor level, the better the stability of the perovskite material. Therefore, the perovskite crystals with HCl additive seem to be more stable, and this provides a simple and effective means to improve the device stability at the material level.

CONCLUSIONS

A simple and efficient method has been developed to improve the quality of perovskite thin film through manipulating PbI_2 thin film crystallization and growth by introducing halogen acid additives, i.e., HCl and HI. With 2.5 vol % HI additive, 30% PCE improvement can be obtained in a planar-heterojunction perovskite solar cell, whereas with 2.5 vol % HCl additive, a high efficiency of 15.2% can be obtained that represents a 58% enhancement. The additives, i.e., HCl and HI but especially HCl, not only improve the perovskite thin film uniformity and coverage on the TiO_2 dense layer but also improve its crystallinity and stability. The latter is an extermely attractive benefit for organic−inorganic hybrid perovskite PV applications.

METHODS

Solar Cell Fabrication. Unless stated otherwise, all fabrication processes were carried out in a glovebox filled with nitrogen and with less than 1% relative humidity level. Devices were fabricated on the laser-etched FTO glass substrates with a sheet resistance of 10−15 Ω square^{-1}. The substrates were cleaned by ultrasonication in soap water, DI water, acetone, and 2-propanol and subjected to an UV−ozone treatment for 30 min. An approximately 30 nm thick dense TiO_2 layer was spin-coated on the substrates by using a 0.15 M titanium isopropoxide (TIP) ethanol solution at a speed of 3000 rpm for 30 s. Subsequently, the sample was calcinated at 450 °C for 2 h, during which time a slow heating-up and cooling-down procedure was adopted.

PbI_2 was dissolved in DMF at a concentration of 461 mg mL^{-1} under stirring at 70 °C, which is maintained during the entire fabrication process. After filtration with a 0.25 μm pore size filter, the PbI_2 layer was deposited by spin-coating on the TiO_2 dense layer coated substrates at 1000−1500 rpm for 30 s and dried at 70 °C for 30 min on a hot plate. Subsequently, upon cooling down to room temperature, the PbI_2-coated substrates were immersed in the organic part CH_3NH_3I solution (30 mg mL^{-1} in 2-propanol) for 90 s to complete the reaction. Finally, a rinsing step with 2-propanol was required for removing the excess organic fraction, and the resulting sample was dried at 90 °C for 60 min.

The HTL was subsequently deposited by spin-coating at a speed of 4000 rpm for 30 s. The HTL solution was prepared by dissolving 79 mg of Spiro-MeOTAD, 28.8 μL of 4-*tert*-butylpyridine, 17.5 μL of a 520 mg mL^{-1} lithium bis(trifluoromethylsulfonyl)imide in acetonitrile in 0.99 mL of chorobenzene. The HTL-coated substrates were kept overnight before depositing the counter electrode.

Finally, a 100 nm layer of silver and a 15 nm layer of MoO_3 were thermally evaporated on top of these devices through the shadow mask with an effective area ranging from 0.1 to 0.25 cm^2. The device area corresponding to the best performance was 0.12 cm^2.

DOI: 10.1021/acsami.5b01049
ACS Appl. Mater. Interfaces 2015, 7, 14614−14619

Device Characterization. Photovoltaic characterization was carried out using a Keithley 2400 digital source meter with scan rate of 0.22 V s^{-1} under illumination of AM1.5G 100 mW cm^{-2} from a solar simulator ABET SUN 2000. When measuring the photovoltaic properties of the device, the mask was used to define the device area. The power density of the solar simulator was calibrated by a silicon reference cell (NIST) and monitored by a power meter throughout the testing. The external quantum efficiency (EQE) values were measured with an EQE system equipped with a xenon lamp (Oriel 66902, 300 W), a monochromator (Newport 66902), a Si detector (Oriel 76175_71580), and a dual-channel power meter (Newport 2931_C).

Absorption measurements were carried by an Agilent Varian Cary 4000UV/VIS/NIR spectrophotometer. The perovskite materials were deposited directly on the TiO_2-coated substrates with measured thickness ranging between 350 and 800 nm. X-ray diffraction (XRD) was performed by Rigaku 9 kW Smartlabusing Cu Kα radiation.

■ ASSOCIATED CONTENT

Supporting Information

Perovskite thin film characterization, such as top-view SEM images for the solution-processed perovskite thin film with HCl additive, XPS analysis on the perovskite layers, among others; solar cell characterization, such as optimization of the devices with additive, hysteresis analysis, and the average perovskite solar cells characteristics. The Supporting Information is available free of charge on the ACS Publications website at DOI: 10.1021/acsami.5b01049.

■ AUTHOR INFORMATION

Corresponding Author

*E-mail: mmwleung@polyu.edu.hk.

Present Addresses

L.Y.: Science and Technology on Surface Physics and Chemistry Laboratory, Mianyang 621907, Sichuan, China.

J.W.: Chinese Academy of Engineering Physics, Mianyang 621907, Sichuan, China.

Notes

The authors declare no competing financial interest.

■ ACKNOWLEDGMENTS

The authors acknowledged the use of Prof. Charles Surya's laboratory in EIE of PolyU for fabricating counter electrodes for the PV devices.

■ REFERENCES

(1) Kojima, A.; Teshima, K.; Shirai, Y.; Miyasaka, T. Organometal Halide Perovskites as Visible-Light Sensitizers for Photovoltaic Cells. *J. Am. Chem. Soc.* **2009**, *131*, 6050−6051.

(2) Kim, H. S.; Lee, C. R.; Im, J. H.; Lee, K. B.; Moehl, T.; Marchioro, A.; Moon, S. J.; Humphry-Baker, R.; Yum, J. H.; Moser, J. E.; Gratzel, M.; Park, N. G. Lead Iodide Perovskite Sensitized All-Solid-State Submicron Thin Flim Mesoscopic Solar Cell with Efficiency Exceeding 9%. *Sci. Rep.* **2012**, *2*, 591−597.

(3) Lee, M. M.; Teuscher, J.; Miyasaka, T.; Murakami, T. N.; Snaith, H. J. Efficient Hybrid Solar Cells Based on Meso-Superstructured Organometal Halide Perovskites. *Science* **2012**, *338*, 643−647.

(4) Burschka, J.; Pellet, N.; Moon, S. J.; Humphry-Baker, R. H.; Gao, P.; Nazeeruddin, M. K.; Gratzel, M. Sequential Deposition as a Route to High-Performance Perovskite-Sensitized Solar Cells. *Nature* **2013**, *499*, 316.

(5) Zhou, H. P.; Chen, Q.; Li, G.; Luo, S.; Song, T.; Duan, H.; Hong, Z. R.; You, J. B.; Liu, Y. S.; Yang, Y. Interface Engineering of Highly Efficient Perovskite Solar Cells. *Science* **2014**, *345*, 542−546.

(6) Green, M. A.; Emery, K.; Hishikawa, Y.; Warta, W.; Dunlop, E. D. Solar Cell Efficiency Tables (Version 45). *Prog. Photovoltaics* **2015**, *23*, 1−9.

(7) Park, N. G. Organometal Perovskite Light Absorbers Towards a 20% Efficiency Low-Cost Solid-State Mesoscopic Solar Cell. *J. Phys. Chem. Lett.* **2013**, *4*, 2423−2429.

(8) Docampo, P.; Hanusch, F.; Stranks, S. D.; Döblinger, M.; Feckl, J. M.; Ehrensperger, M.; Minar, N. K.; Johnston, M. B.; Snaith, H. J.; Bein, T. Solution Deposition-Conversion for Planar Heterojunction Mixed Halide Perovskite Solar Cells. *Adv. Energy Mater.* **2014**, *4*, 1400355−1400359.

(9) Eperon, G. E.; Burlakov, V. M.; Docampo, P.; Goriely, A.; Snaith, H. J. Morphological Control for High Performance, Solution-Processed Planar Heterojunction Perovskite Solar Cells. *Adv. Funct. Mater.* **2014**, *24*, 151−157.

(10) Cai, B.; Xing, Y. E.; Yang, Z.; Zhang, W. H.; Qiu, J. H. High Performance Hybrid Solar Cells Sensitized by Organolead Halide Perovskites. *Energy Environ. Sci.* **2013**, *6*, 1480−1485.

(11) Xu, Y.; Shi, J.; Lv, S.; Zhu, L.; Dong, J.; Wu, H.; Xiao, Y.; Luo, Y.; Wang, S.; Li, D.; Li, X.; Meng, Q. Simple Way to Engineer Metal−Semiconductor Interface for Enhanced Performance of Perovskite Organic Lead Iodide Solar Cells. *ACS Appl. Mater. Interfaces* **2014**, *6*, 5651−5656.

(12) Liu, M. Z.; Johnston, M. B.; Snaith, H. J. Efficient Planar Heterojunction Perovskite Solar Cells by Vapour Deposition. *Nature* **2013**, *501*, 395−398.

(13) Liang, P. W.; Liao, C. Y.; Chueh, C. C.; Zuo, F.; Williams, S. T.; Xin, X. K.; Lin, J. J.; Jen, A. K.Y. Additive Enhanced Crystallization of Solution-Processed Perovskite for Highly Efficient Planar-Heterojunction Solar Cells. *Adv. Mater.* **2014**, *26*, 3748−3754.

(14) Eperon, G. E.; Stranks, S. D.; Menelaou, C.; Johnston, M. B.; Herz, L. M.; Snaith, H. J. Formamidinium Lead Trihalide: a Broadly Tunable Perovskite for Efficient Planar Heterojunction Solar Cells. *Energy Environ. Sci.* **2014**, *7*, 982−988.

(15) Xiao, Z.; Bi, C.; Shao, Y.; Dong, Q.; Wang, Q.; Yuan, Y.; Wang, C.; Gao, Y.; Huang, J. Efficient, High Yield Perovskite Photovoltaic Devices Grown by Inter Diffusion of Solution-Processed Precursor Stacking Layers. *Energy Environ. Sci.* **2014**, *7*, 2619−2623.

(16) Wu, Y.; Islam, A.; Yang, X.; Qin, C.; Liu, J.; Zhang, K.; Peng, W.; Han, L. Retarding the Crystallization of PbI_2 for Highly Reproducible Planar-Structured Perovskite Solar Cells *via* Sequential Deposition. *Energy Environ. Sci.* **2014**, *7*, 2934−2938.

(17) Heo, J. H.; Song, D. H.; Im, S. H. Planar $CH_3NH_3PbBr_3$ Hybrid Solar Cells with 10.4% Power Conversion Efficiency, Fabricated by Controlled Crystallization in the Spin-Coating Process. *Adv. Mater.* **2014**, *26*, 8179−8183.

(18) Liu, D. Y.; Kelly, T. L. Perovskite Solar Cells with a Planar Heterojunction Structure Prepared Using Room-Temperature Solution Processing Techniques. *Nat. Photonics* **2013**, *8*, 133−138.

(19) Zheng, Z.; Liu, A. R.; Wang, S. M.; Wang, Y.; Li, Z. S.; Lau, W. M.; Zhang, L. Z. In Situ Growth of Epitaxial Lead Iodide Films Composed of Hexagonal Single Crystals. *J. Mater. Chem.* **2005**, *15*, 4555−4559.

(20) Snaith, H. J.; Abate, A.; Ball, J. M.; Eperon, G. E.; Leijtens, T.; Noel, N. K.; Stranks, S. D.; Wang, J. T.; Wojciechowski, K.; Zhang, W. Anomalous Hysteresis in Perovskite Solar Cells. *J. Phys. Chem. Lett.* **2014**, *5*, 1511−1515.

(21) Chiang, C. H.; Tseng, Z. L.; Wu, C. G. Planar Heterojunction Perovskite /$PC_{71}BM$ Solar Cells with Enhanced Open Circuit Voltage via a (2/1)-step Spin-coating Process. *J. Mater. Chem. A* **2014**, *2*, 15897−15903.

DOI: 10.1021/acsami.5b01049
ACS Appl. Mater. Interfaces 2015, 7, 14614−14619